Received: 15 July 2023 | Revised: 19 September 2023 | Accepted: 21 September 2023

DOI: 10.1002/ardp.202300387

SHORT COMMUNICATION

ARCH PHARM DPhG
Archiv der Pharmazie

Structural determinants of sphingosine-1-phosphate receptor selectivity

Friederike Wunsch[1] | Trung Ngoc Nguyen[2] | Gerhard Wolber[2] | Marcel Bermudez[1]

[1]Faculty of Chemistry and Pharmacy, Institue for Pharmaceutical and Medical Chemistry, University of Münster, Münster, Germany

[2]Department of Biology, Chemistry and Pharmacy, Institute for Pharmacy, Freie Universität Berlin, Berlin, Germany

Correspondence
Marcel Bermudez, Faculty of Chemistry and Pharmacy, Institute for Pharmaceutical and Medicinal Chemistry, University of Münster, Corrensstr. 48, 48149 Münster, Germany.
Email: m.bermudez@uni-muenster.de

Funding information
Joachim Herz Stiftung; German Research Foundation (Deutsche Forschungsgemeinschaft), Grant/Award Number: 407626949

Abstract

Fingolimod, the prodrug of fingolimod-1-phosphate (F1P), was the first sphingosine-1-phosphate receptor (S1PR) modulator approved for multiple sclerosis. F1P unselectively targets all five S1PR subtypes. While agonism (functional antagonism via receptor internalization) at $S1PR_1$ leads to the desired immune modulatory effects, agonism at $S1PR_3$ is associated with cardiac adverse effects. This motivated the development of $S1PR_3$-sparing compounds and led to a second generation of $S1PR_{1,5}$-selective ligands like siponimod and ozanimod. Our method combines molecular dynamics simulations and three-dimensional pharmacophores (dynophores) and enables the elucidation of S1PR subtype-specific binding site characteristics, visualizing also subtle differences in receptor–ligand interactions. F1P and the endogenous ligand sphingosine-1-phosphate bind to the orthosteric pocket of all S1PRs, but show different binding mode dynamics, uncovering potential starting points for the development of subtype-specific ligands. Our study contributes to the mechanistic understanding of the selectivity profile of approved drugs like ozanimod and siponimod and pharmaceutical tool compounds like CYM5541.

KEYWORDS
drug design, GPCR, molecular dynamics, pharmacophores, selectivity

1 | INTRODUCTION

A major challenge in drug design is the development of selective ligands, in particular, when binding sites are highly conserved within a protein family. While different subtypes typically bind the same or highly similar ligands and share the same architecture, subtle differences can account for specificity. In this study, we focus on the sphingosine-1-phosphate receptor (S1PR) family consisting of five G protein-coupled receptors (GPCRs) that all respond to sphingosine-1-phosphate (S1P) as endogenous agonist. Phylogenetically S1PRs belong to the lipid GPCRs, a subgroup of class A GPCRs. All class A GPCRs share a common architecture of seven transmembrane domains and a common activation mechanism characterized by an allosteric coupling of the ligand-binding pocket and the intracellular receptor region. Receptor activation results in the binding of intracellular binding partners such as different G proteins or the binding of β-arrestin.[1,2] Several S1PR agonists have been approved for the therapy of multiple sclerosis and inflammatory bowel disease.

Like S1P, the active metabolite of the first-in-class drug fingolimod, fingolimod-1-phosphate (F1P), binds to and activates all five S1PR subtypes. Activation of $S1PR_1$ receptors mainly contributes to desired immune-modulatory effects, interestingly, by functional antagonism via receptor internalization.[3,4] However, bioactivity at other S1PR subtypes has been associated with adverse drug effects, most prominently the $S1PR_3$-mediated QT prolongation[5] and the bradycardia observed in mice.[6]

Although the role of $S1PR_3$ for the cardiac side effects in patients has been controversially discussed, it was considered an off-target for the development of new S1PR modulators as immunomodulatory drugs. Second-generation S1PR modulators like siponimod (Spm) or ozanimod (Ozm) target subtypes 1 and 5 only, which makes them clinically preferable.[3,6,7] The protein data bank (PDB) database currently contains structural information of active conformations for all S1PR subtypes except $S1PR_4$. For $S1PR_1$ and $S1PR_5$, X-ray structures of inactive receptor conformations are also available and provide static views of receptor–ligand complexes.[4,8–15] All S1PR subtypes can bind S1P and phosphorylated fingolimod (F1P), but their binding mode dynamics differ and unveil mechanisms by which subtype selectivity might be reached. Here, we used a fully automated combination of molecular dynamics simulations and three-dimensional (3D)-pharmacophores (dynophores)[16–18] to elucidate subtype-specific binding site characteristics of the S1PR family. We focus our analyses on $S1PR_1$ and $S1PR_5$ as they are targeted by second-generation S1PR modulators Spm and Ozm and $S1PR_3$ as an important off-target for S1PR modulators.

2 | RESULTS AND DISCUSSION

All available experimental structures indicate the orthosteric binding site in the core region of the receptor (Figure 1a, Supporting Information: Table S1). All S1P receptor modulators used in this study (Figure 1b, Supporting Information: Figure S1) bind to this site with a highly similar binding orientation, in which the polar head group protrudes to the extracellular loop region and the lipophilic tail points to the receptor core. An interesting exception is the $S1PR_3$-selective ligand CYM5541,[13,19,20] which is described below. Superimposition of active and inactive receptor conformations of $S1PR_1$ suggests the typical activation mechanism for GPCRs that is characterized by an allosteric coupling of the ligand-binding site and the intracellular receptor region with an outward movement of transmembrane helix 6 and an inward movement of TM7 (Supporting Information: Figure S2).[2,12] Initial molecular dynamics simulations with the inactive state of $S1PR_1$ in complex with the antagonist ML056[21] showed a highly stable binding mode with regard to the polar head group but also indicated a high flexibility of the lipophilic tail (Supporting Information: Figure S3). We hypothesized that divergent dynamics of the lipophilic pocket contribute to the subtype selectivity of second-generation S1PR modulators. Therefore, we used classical all-atoms molecular dynamics simulations to analyze subtype-specific differences in binding mode dynamics.

We compared the binding modes and dynamics of S1P and F1P bound to $S1PR_1$, $S1PR_3$, and $S1PR_5$ (Supporting Information: Table S2, Figure S4). While the polar head group showed only low flexibility, the lipophilic tail was found to be more divergent with

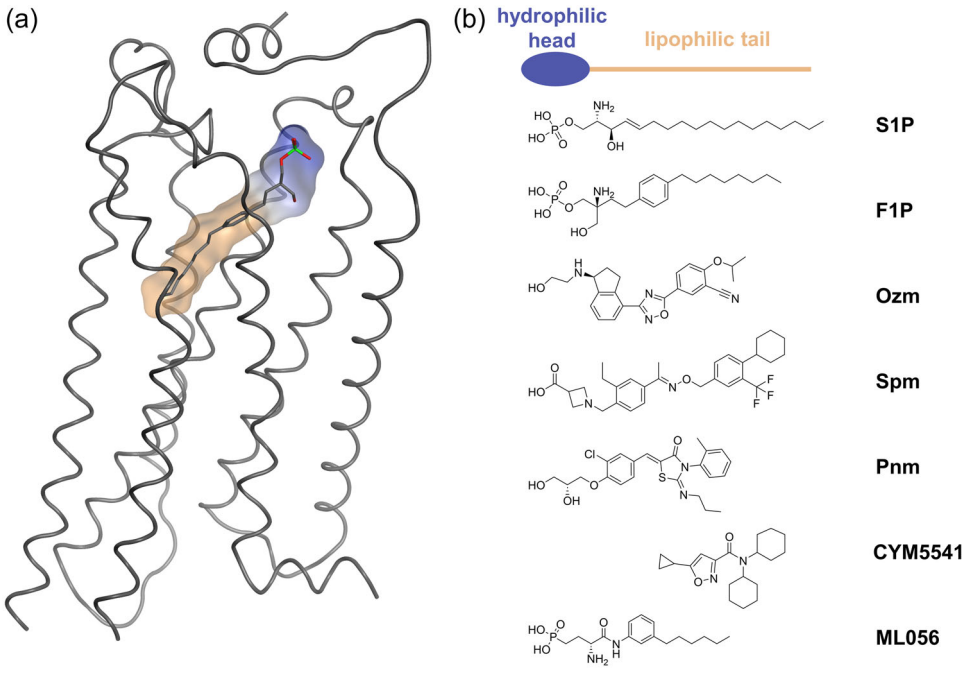

FIGURE 1 (a) Binding site location for S1PR modulators. F1P in the binding site of $S1PR_1$: hydrophilic (blue) and lipophilic (orange) surface. (b) The S1PR ligands used in this study are shown as two-dimensional structures. All of them bind to the same binding site. F1P, fingolimod-1-phosphate; Ozm, ozanimod; S1P, sphingosine-1-phosphate; Spm, siponimod.

regard to the studied subtypes. In $S1PR_3$, we observed a unique dynamic behavior with a branched lipophilic binding pocket (Figure 2a–d). The lipophilic alkyl tail of F1P in complex with $S1PR_3$ was found to be able to occupy two distinct subpockets within the lipophilic binding site, a behavior that was not observed for $S1PR_1$ and $S1PR_5$. Interestingly, this is consistent with the binding mode of $S1PR_3$-selective ligand CYM5541, which has two cyclohexyl moieties that perfectly fit into the two observed orientations of F1P's alkyl tail when bound to $S1PR_3$ (Figure 2b,e). While those two pockets are simultaneously open in $S1PR_3$, only one of them can be accessed in $S1PR_1$ or $S1PR_5$, despite those pockets being larger in those subtypes. Interestingly, these results could not be obtained by static approaches and were only possible by analyzing the dynamics of the binding mode. Supporting Information: Figure S5 shows ligand-dependent rotamers of $F^{5.47}$ in $S1PR_3$, which is involved in F1P's branched behavior. The scaffold of (Spm in $S1PR_1$ and $S1PR_5$) CYM5541 in $S1PR_3$ impairs the rotation of $F^{5.47}$. In the presence of F1P, $F^{5.47}$ can freely rotate toward transmembrane helix 3.

We provide a rational and mechanistic explanation for the selectivity of CYM5541. In the dynamic pharmacophore model, we observe that the perfect shape fit of CYM5541 to the lipophilic pocket is a reason for this ligand's activity even without the polar head group that is found in other S1P receptor modulators and was thought to be essential for receptor activation.

Besides the branched lipophilic pocket in $S1PR_3$, we observed some other subtype-specific binding site characteristics. A direct comparison of subtypes 1, 3, and 5 unveiled a narrow channel for the lipophilic tail in $S1PR_3$ (Figure 3). The dynamic pharmacophore model of F1P bound to $S1PR_3$ reveals only a small spread of the feature point cloud in the middle region of the pocket, indicating a narrow binding site at this location. In this region, there are larger amino acids in $S1PR_3$ (I^{ECL2}, $F^{6.55}$) compared to subtypes 1 and 5 (V^{ECL2}, $L^{6.55}$), which results in a structural bottleneck for ligand binding. The polar head group showed a low flexibility and highly similar interactions for all subtypes and all ligands. With regard to fluctuations in the binding mode, we found $S1PR_5$ to have the most dynamic binding site (Supporting Information: Figure S6). This might explain why second-generation S1PR modulators evade binding to $S1PR_3$ (a considered off-target) but can still activate $S1PR_5$. We validated these findings by running molecular dynamics simulation with an introduced $L^{6.55}F$ mutation in $S1PR_1$ and $S1PR_5$ and $F^{6.55}L$ mutation in $S1PR_3$. As I^{ECL2} (Figure 3) also contributes to the bottleneck in the core region of $S1PR_3$, we additionally calculated molecular dynamics triplicates with the corresponding double mutants ($L^{6.55}F$ and $V^{ECL2}I$ in $S1PR_1$ and $S1PR_5$; $F^{6.55}L$ and $I^{ECL2}V$ in $S1PR_3$) (Supporting Information: Table S3).

The observation that the central part of the $S1PR_3$-binding site is narrower compared to other subtypes can rationally explain the subtype profile of Spm and Ozm. Both drugs bind to and activate only subtypes 1 and 5 (Figure 4a,c). In $S1PR_3$, the phenylethyl group of Spm would clash with I^{ECL2} and $I^{7.39}$, and the 2,3-dihydro-1*H*-inden moiety of Ozm would clash with L^{ECL2}, $F^{3.33}$, and $I^{7.39}$ (Figure 4b,d). The absence of $S1PR_3$ activation might be the reason for Ozm and Spm leading less frequently to bradycardia and conduction abnormalities compared to fingolimod.[5,22,23] However, $S1PR_2$, which is also expressed in the heart in a smaller amount and is not targeted by the second-generation S1PR modulators but by F1P, might also contribute to this clinical outcome.[24]

In addition, fingolimod is a prodrug, which needs to be phosphorylated by sphingosine-kinases to the bioactive form F1P and might be less controllable in the initial therapeutic phase than the second-generation S1PR modulators. For Spm and Ozm, a dose titration during therapy initiation is manageable more easily and independent from individual bioactivation rates, which might play a role in reducing $S1PR_1$-mediated heart rate decrease.[25]

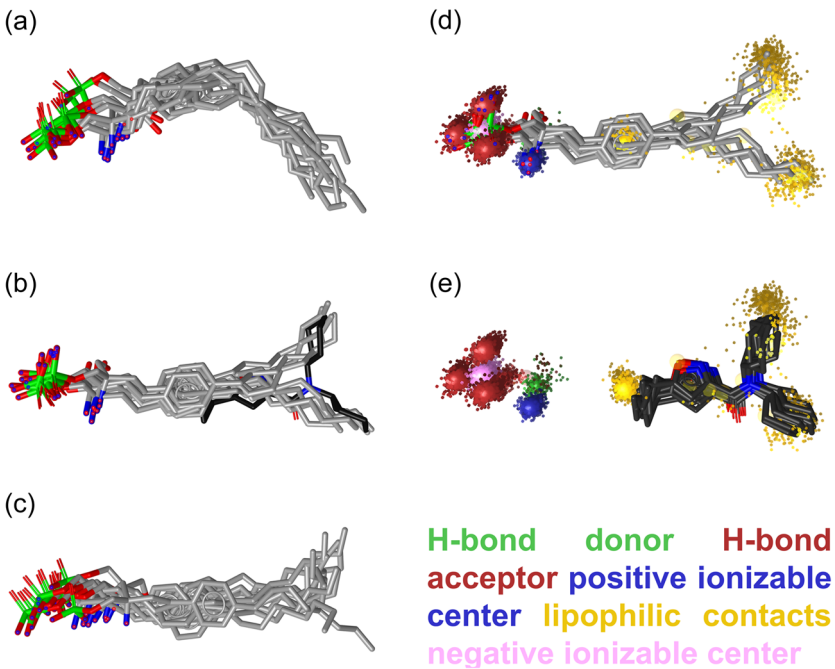

FIGURE 2 Binding mode dynamics unveil a unique possibility to target $S1PR_3$. (a) Superposition of every 100th frame of the F1P trajectory in $S1PR_1$. (b) Superposition of every 100th frame of the F1P trajectory in $S1PR_3$ unveils a dynamic binding mode and branched lipophilic binding pocket in $S1PR_3$, which perfectly fits the $S1PR_3$-selective ligand CYM5541 (dark gray). A ligand superimposition shows structural overlaps of both ligands. (c) Superposition of every 100th frame of the F1P trajectory in $S1PR_5$. (d) The dynophore of F1P in $S1PR_3$ clearly indicates two possible orientations of the lipophilic tail, which is in accordance with (e) the binding mode dynamics of CYM5541. F1P, fingolimod-1-phosphate; S1PR, sphingosine-1-phosphate receptor.

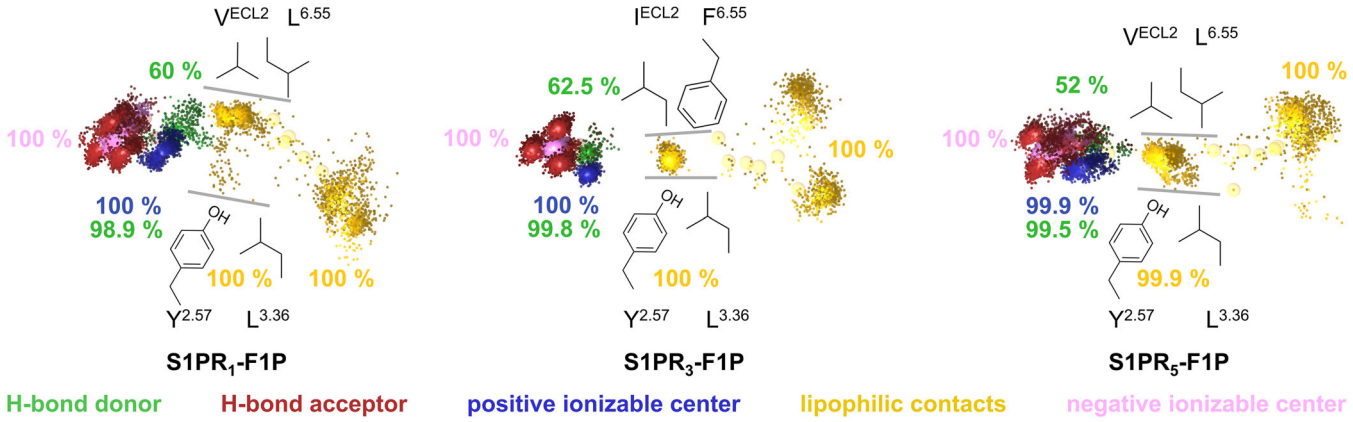

FIGURE 3 The center of the $S1PR_3$-binding site is narrower compared to other subtypes. Dynophores of F1P indicate a very similar interaction pattern for the polar head group but differences in the spatiotemporal behavior of the lipophilic tail. We observed a narrower center (indicated by gray lines) for the $S1PR_3$ compared to other subtypes. The percentages next to the features refer to their average occurrence frequency in three simulations. For clarity, the percentages for the hydrogen bond acceptors in red have been omitted. F1P, fingolimod-1-phosphate; S1PR, sphingosine-1-phosphate receptor.

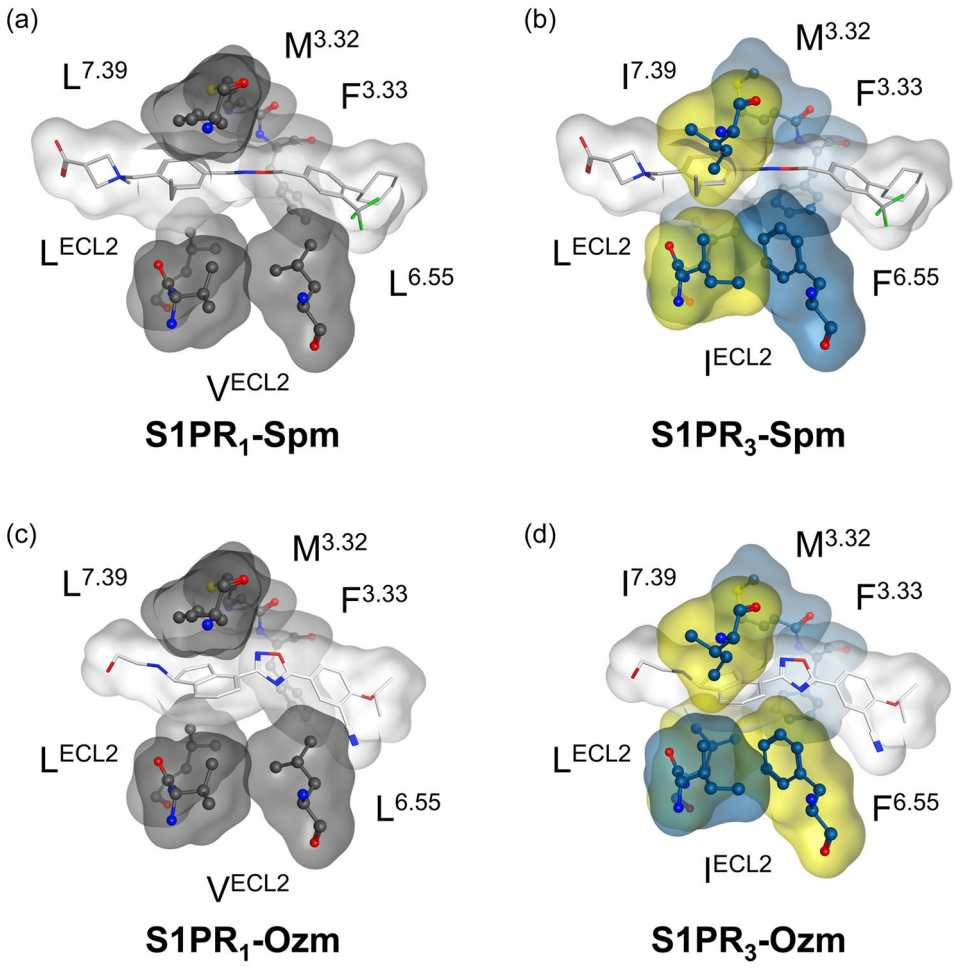

FIGURE 4 The structural bottleneck in $S1PR_3$. Spm and Ozm perfectly fit to the binding site of $S1PR_1$ [(a) and (c), gray residues] but are incompatible with binding to $S1PR_3$ [(b) and (d), blue residues]. Residues with a yellow surface show atom clashes. Ozm, ozanimod; S1PR, sphingosine-1-phosphate receptor; Spm, siponimod.

Moreover, fingolimod shows a comparatively long half-life and is clinically less controllable than the newer derivatives like Spm or ponesimod (Pnm). In the case of Ozm, the active metabolites CC1084307 and CC112273 (of the oxidative dealkylation of the ((2,3-dihydro-1*H*-inden-1-yl)amino)ethanol group) must be considered, which also have a long half-life and show a high activity at $S1PR_1$ and $S1PR_5$.[25,26]

We conclude that sterically demanding moieties in the central part of the binding pocket are incompatible with $S1PR_3$ binding, providing a general design principle for S1PR modulators without $S1PR_3$ activity. This explanation is compatible with the selectivity profile of other S1P modulators that were approved later or are used as pharmacological tools. Pnm, cenerimod,[27] and SEW2871[28] all have a sterically demanding lipophilic building block that is incompatible with the narrow central part of the binding site of $S1PR_3$ and evades activity at this receptor subtype (Supporting Information: Figure S7).

3 | CONCLUSION

In summary, we provide a rational explanation for the subtype profile of clinically relevant S1PR modulators (F1P, Spm, Ozm, and Pnm) and specific pharmacological tools (CYM5541 and SEW2871). We demonstrate the applicability of a dynamic pharmacophore approach to unveil and analyze also subtle differences, which only occur when receptors are considered as dynamic entities.

4 | EXPERIMENTAL

Structural and dynamic modeling of S1P receptor–ligand complexes was based on structural information from the following PDB entries: 7TD3 ($S1PR_1$-S1P),[9] 7TD4 ($S1PR_1$-Spm),[9] 7VIF ($S1PR_1$-F1P),[11] 7EW0 ($S1PR_1$-Ozm),[12] 7EW1 ($S1PR_5$-Spm),[12] 7EW2 ($S1PR_3$-F1P),[13] 7EW3 ($S1PR_3$-S1P),[13] 7EW4 ($S1PR_3$-CYM5541),[13] and 3V2Y (inactive $S1PR_1$-ML056).[8] All structural models were prepared using molecular operating environment (MOE) 2020.0901.[29] Missing side chains and loops were added, and atom clashes were eliminated. All docking experiments were performed with GOLD 5.2[30] by using default settings and goldscore as primary scoring function. Mutations in position 6.55 (corresponding to L276F in $S1PR_1$, F263L in $S1PR_3$, and L271F in $S1PR_5$) and in ECL2 (corresponding to V194I in $S1PR_1$, I188V in $S1PR_3$, and V185I in $S1PR_5$) were built with the mutation tool in MOE; side chains were manually adapted and minimized to optimize geometries. 3D pharmacophore models built with LigandScout 4.4.3 were used to select the most plausible docking poses. S1P, F1P, and Ozm were positioned in 7EW1 (S1PR5) by superpositioning with the corresponding S1PR1–ligand complex as template for the docking experiments.

Molecular dynamics simulations were prepared in Maestro 12.7.156.[31] Each GPCR–ligand complex was titrated to pH 7 and solvated in SPC water[32] and 0.15 M NaCl. The system was placed in an orthorhombic box, with a 10 Å distance to each receptor site, and periodic boundary conditions were applied. According to the transmembrane residues given on the orientations of proteins in membranes database (OPM) website,[33] the protein was placed in a pre-equilibrated POPC membrane (palmitoyl-oleoyl-phosphatidylcholine bilayer). As no OPM entry was given for $S1PR_5$, the transmembrane residues were determined by superpositioning with $S1PR_1$. The optimized potentials for liquid simulations-all atom force field[34] was used to parameterize the system. Molecular dynamics simulations were performed with Desmond-v6.5[35] on local GPUs (RTX A5000) for 100 ns in triplicates. Temperature and pressure were kept constant at 300 K and atmospheric pressure, respectively, while the number of particles in each system was kept constant. Since no reasonable docking pose for Spm and Ozm could be found in $S1PR_3$, ligands were placed by superpositioning with the corresponding $S1PR_1$–ligand complexes. Statistics of F1P conformations in $S1PR_3$ and $S1PR_5$ were done by sorting conformations using visual molecular dynamics (VMD).

The obtained trajectories were analyzed using VMD 1.9.3.[36] Therefore, the backbone's heavy atoms of each trajectory frame were aligned to those of frame 1 (atomic deviations are reported in Supporting Information: Tables S4 and S5). Dynamic pharmacophore models were generated with the dynophore application[37,38] as integrated in the framework of Ligand Scout 4.4.3.[35,36] root-mean-square deviation plots for the pocket residues, as indicated in Supporting Information: Figure S1, were calculated based on the first frame of the trajectory with all heavy atoms included; values for each triplicate were merged before violin plotting.[39]

PDB entries 7EW7 ($S1PR_1$-SEW2871),[12] 7EVZ ($S1PR_1$-cenerimod),[12] and 7TD4[9] with docked Pnm were used for static pharmacophore calculations also using Ligand Scout 4.4.3.

ACKNOWLEDGMENTS

We thank the German Research Foundation (DFG 407626949) for the financial support of F. W. and M. B. All authors are members of the COST Action CA18133 (ERNEST). M. B. thanks the Joachim Herz Foundation for the financial support. Open Access funding enabled and organized by Projekt DEAL.

CONFLICTS OF INTEREST STATEMENT

The authors declare no conflicts of interest.

ORCID

Gerhard Wolber http://orcid.org/0000-0002-5344-0048
Marcel Bermudez http://orcid.org/0000-0002-7421-3282

REFERENCES

[1] D. Yang, Q. Zhou, V. Labroska, S. Qin, S. Darbalaei, Y. Wu, E. Yuliantie, L. Xie, H. Tao, J. Cheng, Q. Liu, S. Zhao, W. Shui, Y. Jiang, M.-W. Wang, *Signal Tranduct. Target. Ther.* **2021**, *6*, 7.
[2] A. Bock, M. Bermudez, *FEBS. J.* **2021**, *288*, 2513.
[3] R. Roy, A. A. Alotaibi, M. S. Freedman, *CNS Drugs* **2021**, *35*, 385.

[4] H. Chen, K. Chen, W. Huang, L. M. Staudt, J. G. Cyster, X. Li, *Sci. Adv.* **2022**, *8*, eabn0067.

[5] J. Q. Tran, J. P. Hartung, A. D. Olson, B. Mendzelevski, G. A. Timony, M. F. Boehm, R. J. Peach, S. Gujrathi, P. A. Frohna, *Clin. Pharmacol. Drug Dev.* **2018**, *7*, 263.

[6] P. Gergely, B. Nuesslein-Hildesheim, D. Guerini, V. Brinkmann, M. Traebert, C. Bruns, S. Pan, N. Gray, K. Hinterding, N. Cooke, A. Groenewegen, A. Vitaliti, T. Sing, O. Luttringer, J. Yang, A. Gardin, N. Wang, W. J. Crumb, Jr., M. Saltzman, M. Rosenberg, E. Wallström, *Br. J. Pharmacol.* **2012**, *167*, 1035.

[7] J. V. Selkirk, A. Bortolato, Y. G. Yan, N. Ching, R. Hargreaves, *Front. Pharmacol.* **2022**, *13*, 892097.

[8] M. A. Hanson, C. B. Roth, E. Jo, M. T. Griffith, F. L. Scott, G. Reinhart, H. Desale, B. Clemons, S. M. Cahalan, S. C. Schuerer, M. G. Sanna, G. W. Han, P. Kuhn, H. Rosen, R. C. Stevens, *Science* **2012**, *335*, 851.

[9] S. Liu, N. Paknejad, L. Zhu, Y. Kihara, M. Ray, J. Chun, W. Liu, R. K. Hite, X.-Y. Huang, *Nat. Commun.* **2022**, *13*, 731.

[10] E. Lyapina, E. Marin, A. Gusach, P. Orekhov, A. Gerasimov, A. Luginina, D. Vakhrameev, M. Ergasheva, M. Kovaleva, G. Khusainov, P. Khorn, M. Shevtsov, K. Kovalev, S. Bukhdruker, I. Okhrimenko, P. Popov, H. Hu, U. Weierstall, W. Liu, Y. Cho, I. Gushchin, A. Rogachev, G. Bourenkov, S. Park, G. Park, H. J. Hyun, J. Park, V. Gordeliy, V. Borshchevskiy, A. Mishin, V. Cherezov, *Nat. Commun.* **2022**, *13*, 4736.

[11] L. Yu, L. He, B. Gan, R. Ti, Q. Xiao, X. Yang, H. Hu, L. Zhu, S. Wang, R. Ren, *Proc. Natl. Acad. Sci. USA* **2022**, *119*, e2117716119.

[12] Y. Yuan, G. Jia, C. Wu, W. Wang, L. Cheng, Q. Li, Z. Li, K. Luo, S. Yang, W. Yan, Z. Su, Z. Shao, *Cell Res.* **2021**, *31*, 1263.

[13] C. Zhao, L. Cheng, W. Wang, H. Wang, Y. Luo, Y. Feng, X. Wang, H. Fu, Y. Cai, S. Yang, P. Fu, W. Yan, Z. Shao, *Cell Res.* **2022**, *32*, 218.

[14] S. Maeda, Y. Shiimura, H. Asada, K. Hirata, F. Luo, E. Nango, N. Tanaka, M. Toyomoto, A. Inoue, J. Aoki, S. Iwata, M. Hagiwara, *Sci. Adv.* **2021**, *7*, eabf5325.

[15] H. Chen, Y. Qin, M. Chou, J. G. Cyster, X. Li, *eLife* **2023**, *12*, e88204.

[16] A. Bock, M. Bermudez, F. Krebs, C. Matera, B. Chirinda, D. Sydow, C. Dallanoce, U. Holzgrabe, M. de Amici, M. J. Lohse, G. Wolber, K. Mohr, *J. Biol. Chem.* **2016**, *291*, 16375.

[17] D. Schaller, D. Šribar, T. Noonan, L. Deng, T. N. Nguyen, S. Pach, D. Machalz, M. Bermudez, G. Wolber, *Wiley Interdiscip. Rev.: Comput. Mol. Sci.* **2020**, *10*, e1468.

[18] D. Sydow, *Master Thesis*, Humboldt-Universität zu Berlin (Berlin) **2015**.

[19] M. Guerrero, R. Poddutoori, M. Urbano, X. Peng, T. P. Spicer, P. S. Chase, P. S. Hodder, M.-T. Schaeffer, S. Brown, H. Rosen, E. Roberts, *Bioorg. Med. Chem. Lett.* **2013**, *23*, 6346.

[20] S. C. Schürer, S. J. Brown, P. J. Gonzalez-Cabrera, M.-T. Schaeffer, J. Chapman, E. Jo, P. Chase, T. Spicer, P. Hodder, H. Rosen, *ACS Chem. Biol.* **2008**, *3*, 486.

[21] M. G. Sanna, S.-K. Wang, P. J. Gonzalez-Cabrera, A. Don, D. Marsolais, M. P. Matheu, S. H. Wei, I. Parker, E. Jo, W.-C. Cheng, M. D. Cahalan, C. H. Wong, H. Rosen, *Nat. Chem. Biol.* **2006**, *2*, 434.

[22] E. Swallow, O. Patterson-Lomba, L. Yin, R. Mehta, C. Pelletier, D. Kao, J. K. Sheffield, T. Stonehouse, J. Signorovitch, *J. Comp. Eff. Res.* **2020**, *9*, 275.

[23] L. J. Scott, *CNS Drugs* **2020**, *34*, 1191.

[24] D. Mazurais, P. Robert, B. Gout, I. Berrebi-Bertrand, M. P. Laville, T. Calmels, *J. Histochem. Cytochem.* **2002**, *50*, 661.

[25] J. Chun, G. Giovannoni, S. F. Hunter, *Drugs* **2021**, *81*, 207.

[26] J. V. Selkirk, Y. G. Yan, N. Ching, K. Paget, R. Hargreaves, *Eur. J. Pharmacol.* **2023**, *941*, 175442.

[27] L. Piali, M. Birker-Robaczewska, C. Lescop, S. Froidevaux, N. Schmitz, K. Morrison, C. Kohl, M. Rey, R. Studer, E. Vezzali, P. Hess, M. Clozel, B. Steiner, M. H. Bolli, O. Nayler, *Pharmacol. Res. Perspect.* **2017**, *5*, e00370.

[28] J. J. Hale, C. L. Lynch, W. Neway, S. G. Mills, R. Hajdu, C. A. Keohane, M. J. Rosenbach, J. A. Milligan, G.-J. Shei, S. A. Parent, G. Chrebet, J. Bergstrom, D. Card, M. Ferrer, P. Hodder, B. Strulovici, H. Rosen, S. Mandala, *J. Med. Chem.* **2004**, *47*, 6662.

[29] Molecular Operating Environment (MOE). Chemical Computing Group ULC, 910-1010 Sherbrooke St. W., Montreal, QC H3A 2R7, Canada, **2021**.

[30] G. Jones, P. Willett, R. C. Glen, A. R. Leach, R. Taylor, *J. Mol. Biol.* **1997**, *267*, 727.

[31] Schrödinger Release 2021-1. Maestro, Schrödinger, LLC, New York, NY, **2021**.

[32] J. Zielkiewicz, *J. Chem. Phys.* **2005**, *123*, 104501.

[33] M. A. Lomize, I. D. Pogozheva, H. Joo, H. I. Mosberg, A. L. Lomize, *Nucleic Acids Res.* **2012**, *40*, D370.

[34] W. L. Jorgensen, D. S. Maxwell, J. Tirado-Rives, *J. Am. Chem. Soc.* **1996**, *118*, 11225.

[35] K. J. Bowers, E. Chow, H. Xu, R. O. Dror, M. P. Eastwood, B. A. Gregersen, J. L. Klepeis, I. Kolossvary, M. A. Moraes, F. D. Sacerdoti, J. K. Salmon, Y. Shan, D. E. Shaw, *Proceedings of the ACM/IEEE Conference on Supercomputing (SC06)*, Tampa, Florida, November 11-17, **2006**.

[36] W. Humphrey, A. Dalke, K. Schulten, *J. Mol. Graphics* **1996**, *14*, 33.

[37] G. Wolber, A. A. Dornhofer, T. Langer, *J. Comput.-Aided Mol. Des.* **2006**, *20*, 773.

[38] G. Wolber, T. Langer, *J. Chem. Inf. Model.* **2005**, *45*, 160.

[39] T. L. Weissgerber, M. Savic, S. J. Winham, D. Stanisavljevic, V. D. Garovic, N. M. Milic, *J. Biol. Chem.* **2017**, *292*, 20592.

SUPPORTING INFORMATION

Additional supporting information can be found online in the Supporting Information section at the end of this article.

How to cite this article: F. Wunsch, T. N. Nguyen, G. Wolber, M. Bermudez, *Arch. Pharm.* **2023**;*356*:e2300387. https://doi.org/10.1002/ardp.202300387